Dynamical localization in quasiperiodic driven systems

G. Abal,* R. Donangelo,† A. Romanelli, A. C. Sicardi Schifino,‡ and R. Siri
Instituto de Física, Facultad de Ingeniería, Universidad de la República, CC 30, C. P. 11000, Montevideo, Uruguay
(Received 14 November 2001; published 11 April 2002)

We investigate how the time dependence of the Hamiltonian determines the occurrence of dynamical localization (DL) in driven quantum systems with two incommensurate frequencies. If both frequencies are associated to impulsive terms, DL is permanently destroyed. In this case, we show that the evolution is similar to a decoherent case. On the other hand, if both frequencies are associated to smooth driving functions, DL persists although on a time scale longer than in the periodic case. When the driving function consists of a series of pulses of duration σ, we show that the localization time increases as σ^{-2} as the impulsive limit, $\sigma \to 0$, is approached. In the intermediate case, in which only one of the frequencies is associated to an impulsive term in the Hamiltonian, a transition from a localized to a delocalized dynamics takes place at a certain critical value of the strength parameter. We provide an estimate for this critical value, based on analytical considerations. We show how, in all cases, the frequency spectrum of the dynamical response can be used to understand the global features of the motion. All results are numerically checked.

DOI: 10.1103/PhysRevE.65.046236 PACS number(s): 05.45.−a, 03.65.−w, 24.60.Lz, 72.15.Rn

I. INTRODUCTION

Dynamical localization (DL), discovered numerically in 1979 [1], has attracted a great deal of attention after its experimental realization in samples of cold atoms interacting with a far-detuned standing wave of laser light [2]. When the light field is switched on and off periodically, the system can be modeled by the kicked rotor Hamiltonian in a regime in which quantum effects are important [3,4]. This notable series of experiments confirmed previous expectations regarding DL in periodically driven quantum systems. More recently, it has been reported [5] that the addition of a second driving frequency, incommensurate with the first, results in the destruction of DL in the experimentally accessible time scale. The important conceptual issue of whether the addition of a second incommensurate frequency permanently destroys DL or just causes a substantial increase in the localization time, cannot be resolved experimentally. On the other hand, numerical experiments alone are intrinsically unable to distinguish between a very large increase in localization time and an effective suppression of DL. Thus, some theoretical insight on DL for nonperiodically driven systems is presently required in order to provide an answer to this kind of question.

Most theoretical work on the subject has dealt with the special case of periodically driven systems [6,7]. In comparison, little is known on the quantum dynamics of driven systems when the external field is not periodic. In this work we present a basic theoretical framework that may lead to a deeper understanding of DL and quantum diffusion in quasiperiodic systems. Our approach focuses in the relation between the density of the Fourier spectrum of the dynamical response and the localized or diffusive character of the quantum motion. As we shall see, the importance of the impulsive or nonimpulsive character of the driving has been underestimated in the past, since it is at least as important for DL as the number of independent frequencies in the Hamiltonian. Our conclusions are supported by numerical simulations of several characteristic systems.

In Sec. II, a kicked rotor with two driving frequencies is introduced and it is shown that DL is impossible in this system unless the frequencies are commensurable. We also introduce here an energy balance that will be of great importance in the following sections. In Sec. III, a quasiperiodic driven rotor without impulsive terms in the Hamiltonian is discussed. It is shown that, in this kind of system, DL takes place for arbitrary driving strengths provided that the classical analog is chaotic. In Sec. IV, an intermediate system, the modulated kicked rotor, is considered in detail. In this kind of multifrequency system, one driving frequency is associated with the impulsive term and the other with a smoothly varying modulation factor. This system has a transition, from localized to diffusive dynamics, for kicking strengths above a certain threshold. We show how this transition can be understood within our theoretical framework and provide a concrete estimate for the threshold value for the particular example that we consider. Finally, in Sec. V we present a unifying discussion of these results and summarize our conclusions.

II. TWO-FREQUENCY QUANTUM KICKED ROTOR

Let us consider a quantum kicked rotor (QKR) to which a second series of periodic δ kicks is applied. External kicks occur at times $t=nT_1$ and $t=mT_2$, respectively (n,m integers) and we write the Hamiltonian as

$$H=\frac{P^2}{2I}+\cos\theta\left[K_1\sum_{n=1}^{\infty}\delta(t-nT_1)+K_2\sum_{m=1}^{\infty}\delta(t-mT_2)\right], \quad (1)$$

*Electronic address: abal@fing.edu.uy
†Permanent address: Instituto de Física, Universidade Federal do Rio de Janeiro, Caixa Postal 68528, 21945-970 Rio de Janeiro, Brazil.
‡Also at Instituto de Física, Facultad de Ciencias.

where I is the moment of inertia of the rotor, P the angular momentum operator, and K_1 (K_2) the strength parameter for the series of kicks of periods T_1 (T_2). The rational or irrational character of the ratio $r=T_2/T_1$ determines whether the Hamiltonian (1) is periodic or quasiperiodic.

In the angular momentum representation, $P|\ell\rangle=\ell\hbar|\ell\rangle$, the wave vector is $|\Psi(t)\rangle=\Sigma_{\ell=-\infty}^{\infty}a_\ell(t)|\ell\rangle$ and the average energy is $E(t)=\langle\Psi|H|\Psi\rangle=\Sigma_{\ell=-\infty}^{\infty}E_\ell|a_\ell(t)|^2$, where $E_\ell=\ell^2\hbar^2/2I$ are the eigenvalues of $P^2/2I$. As in the case of the QKR, a quantum map

$$a_\ell(t_{n+1})=\sum_{j=-\infty}^{\infty} i^{-(j-\ell)}\exp[-iE_j\Delta t_n/\hbar]J_{j-\ell}(\kappa_n)a_j(t_n) \tag{2}$$

is readily obtained from the Hamiltonian (1). In Eq. (2), we refer to the instant immediately after the nth kick as t_n and to the time interval between two consecutive kicks as $\Delta t_n \equiv t_{n+1}-t_n$. The argument of the kth order cylindrical Bessel function J_k is the dimensionless kick strength $\kappa_n\equiv K_n/\hbar$ that, for this system, takes only the two values ($K_1/\hbar$ or $K_2/\hbar$) depending on the kind of the $(n+1)$th kick. We will use $T\equiv T_1$ as the unit of time.

After a straightforward calculation involving the map (2), the energy increase due to the $(n+1)$th kick can be expressed as

$$E(n+1)-E(n)=\frac{\hbar^2}{2I}\left[\frac{\kappa_n^2}{2}+\Gamma_n\right] \tag{3}$$

with

$$\Gamma_n\equiv 2\kappa_n \mathcal{I}m\sum_{j=-\infty}^{\infty}\left(j+\frac{1}{2}\right)a_j(t_n)a_{j+1}^*(t_n)\times\exp\left[-\frac{i}{\hbar}(E_{j+1}-E_j)\Delta t_n\right] -\frac{\kappa_n^2}{2}\mathrm{Re}\sum_{j=-\infty}^{\infty}a_j(t_n)a_{j+2}^*(t_n)\times\exp\left[-\frac{i}{\hbar}(E_{j+2}-E_j)\Delta t_n\right]. \tag{4}$$

The ensemble average of Eq. (3) is proportional to the diffusion rate in angular momentum, $D_n=\overline{\Delta P_n^2}/T$, if the kick number n is used as a measure of time. The amplitude-independent term in Eq. (3) corresponds to the quasilinear approximation to the classical diffusion coefficient [8],

$$D_{ql}=\frac{\overline{\kappa^2}}{2}, \tag{5}$$

where $\overline{\kappa^2}$ stands for the average value of κ_n^2. The remaining terms, grouped as Γ_n in Eq. (3), depend on the wave vector $\{a_\ell\}$ and on the time interval between kicks. In sum, the energy balance in Eq. (3), contains two qualitatively different terms: one due to classical diffusion and the other (Γ_n) associated to quantum interference effects.

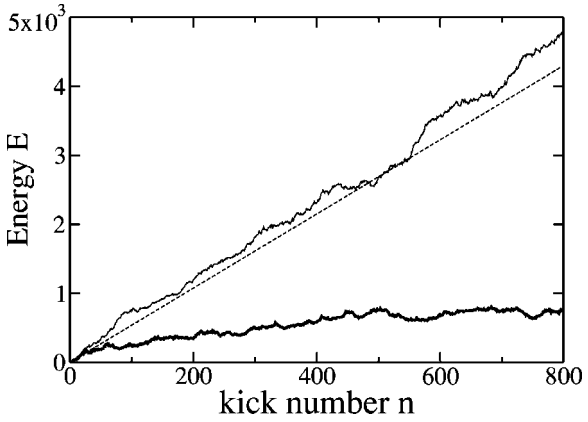

FIG. 1. Energy (in units of $\hbar^2/2I$) as a function of the kick number n for the two-frequency quantum kicked rotor. The evolution was generated from the map (2) with $\kappa=3.279$ and $\xi=1.525$. Two values of the period ratio $r\equiv T_2/T_1$ are shown: $r=3/2$ (thick line) and $r=\sqrt{2}$ (thin line). The dashed line corresponds to the quasilinear approximation, Eq. (5). The initial state was taken to be $|\ell=0\rangle$.

If the terms in Γ_n have random phases, the sums are decoherent, and thus have negligible mean values. Therefore, $\overline{\Gamma_n}=0$ and the system mimics a classical evolution, and the average energy increases linearly with the number of kicks with a slope given by Eq. (5). On the other hand, when DL takes place, the average value of the sums in Γ_n must cancel out the independent term in Eq. (3) , so $\overline{\Gamma_n}=-\overline{\kappa^2}/2$. This can happen only if these sums are coherent. Thus, the long time persistence of correlations among the amplitudes a_ℓ, taken at a given time, is a necessary condition for DL to take place. We emphasize this rather obvious fact because it plays a fundamental role in the discussions in the rest of this paper.

We have performed a numerical study of the two-frequency quantum kicked rotor described by the map (2) with $K_1=K_2$. We write the two dimensionless parameters of the standard QKR model as $\kappa=K/\hbar$ and $\xi=\hbar T/I$. The period ratio, $r\equiv T_2/T_1$, is an additional parameter present in the two-frequency version.

In Fig. 1, we show the evolution of the energy of the rotor for a rational and irrational ratio of the two periods $r\equiv T_2/T_1$. In the first case, the behavior is similar to the usual one-frequency kicked rotor and the energy initially increases in a diffusive way and then, after a characteristic time, it localizes. In the second case, the results strongly suggest that the diffusive behavior continues indefinitely and that in this case dynamical localization does not take place. In fact, we have checked that the energy increases at a rate consistent with the quasilinear approximation to the classical diffusion coefficient, Eq. (5), for at least 10^4 kicks (see Fig. 2).

The results obtained for rational r could be expected because, in this case, the system is equivalent to a kicked rotor with a periodic train of pulses. For an irrational r, our results can be better understood by considering a random rotor, defined as a kicked rotor for which kicks of fixed strength κ are applied at uniformly distributed random time intervals. In

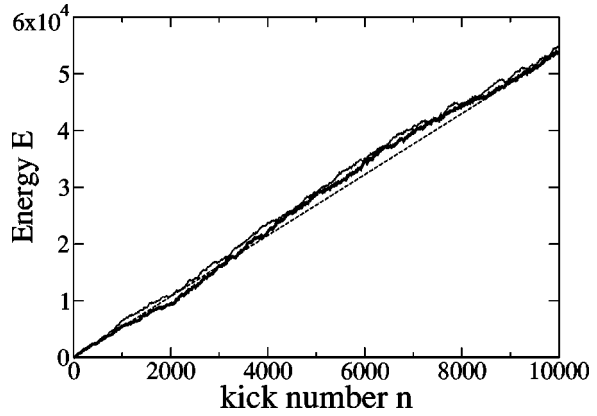

FIG. 2. Energy (in units of $\hbar^2/2I$) as a function of the kick number, n, for the random rotor defined in the text (thick line) and the two-frequency kicked rotor with $r=\sqrt{2}$ (thin line). The dashed line, parameters, and initial conditions are the same as those in Fig. 1.

this case, the map (2) still holds, but the time interval between consecutive kicks Δt_n, is now a random variable uniformly distributed in $[0,T]$. In Fig. 2, we compare the long time evolution of the average energy of this random rotor with the corresponding quasiperiodic kicked rotor. The evolution of the energy is essentially the same in both cases and this suggests that the underlaying dynamics is very similar.

In the case of the quasiperiodic QKR, the time sequence Δt_n is obtained from a systematic rule, once the period ratio r has been specified. In spite of this, all time intervals in this sequence occur only once and as $n\to\infty$ the values of Δt_n are dense and uniformly distributed in $[0,T]$, as is the case for random time intervals. In both cases, numerical results confirm that $\overline{\Gamma_n}\approx 0$ and that classical-like diffusion takes place indefinitely. The effect of these time intervals on the dynamics can be made more explicit by rewriting the map (2) in terms of the initial condition,

$$a_\ell(t_{n+1}) = \sum_{j_1, j_2 \cdots j_{n+1}} i^{-(j_1-\ell)} \exp\left[-\frac{i}{\hbar} \sum_{m=1}^{n+1} E_{j_m} \Delta t_m \right] \times J_{j_{n+1}-\ell}(\kappa_n) J_{j_n - j_{n+1}}(\kappa_{n-1}) \cdots \times J_{j_1 - j_2}(\kappa_0) a_{j_1}(t_0). \tag{6}$$

This expression can be applied to any of the systems discussed so far (periodic, quasiperiodic, and random). The only difference between the localized and the diffusive cases is in the sequence of time intervals Δt_n. In the familiar periodic case, when all time intervals are the same, it is well known that the amplitudes a_ℓ are exponentially localized. When they are substituted in Eq. (3) a coherent sum results in Γ_n, which, as mentioned before, cancels on the average the classical diffusion coefficient and results in a null mean energy increase. On the other hand, in the quasiperiodic case, the phases $-(i/\hbar)\Sigma_{m=1}^{n+1} E_{j_m} \Delta t_m \pmod{2\pi}$, appearing in Eq. (6), form a dense, pseudorandom set in $[0,2\pi]$. When the resulting amplitudes a_ℓ are substituted in Eq. (3), they result in a negligible decoherent sum in Γ_n and the classical diffusion coefficient is obtained.

It is interesting to remark that the previous discussion could have been expressed equally well in terms of the Fourier frequencies associated to the dynamics. In the quasiperiodic case, the time intervals between consecutive kicks are of the form

$$\Delta t_n = |pT_1 - qT_2| = \frac{2\pi}{\omega_1 \omega_2} |p\omega_2 - q\omega_1|, \tag{7}$$

where p and q are arbitrary integers and $\omega_{1,2}=2\pi/T_{1,2}$. These time intervals are dense in $[0,T]$. The corresponding frequencies, $\omega_{pq} \equiv |p\omega_2 - q\omega_1|$, also form a dense set in $[0,\omega_2]$. In other words, all frequencies are relevant for the dynamics and the time evolution of the energy mimics the classical chaotic diffusion, because the average separation between adjacent frequencies, $\Delta\omega$ is null. It is well known that in the periodic QKR, DL is related to the discrete nature of the quasienergy spectrum or, equivalently, to the frequency spectrum of the dynamical response. In fact, this spectrum is discrete in spite that a classical chaotic system has a continuous frequency spectrum. However, due to the uncertainty principle, this discreteness does not manifest itself until a finite time of the order of $1/\Delta\omega$, where $\Delta\omega$ is the average separation between adjacent frequencies. For shorter times, the dynamical evolution ''mimics'' classical diffusion, i.e., quantum diffusion takes place. At larger times, for which the discrete nature of the spectrum becomes manifest, the motion is exponentially localized [7]. A similar argument for the quasiperiodic two-frequency kicked rotor leads us to conclude that in this case, in which $\Delta\omega=0$, the localization time is infinite or, alternatively, that the addition of a second incommensurable frequency permanently destroys DL in impulsive systems, such as the QKR.

III. NONIMPULSIVE SYSTEMS

In the preceding section, we have shown that quantum diffusion takes place for ever in a quasiperiodic kicked rotor in which the driving function has two impulsive components. In this section, we consider the diffusive properties of smoothly driven quantum systems with two frequencies ω_1 and ω_2.

As an example, consider a rotor in which the driving force consists of two series of periodic narrow pulses. Such a system is described by the Hamiltonian

$$H = \frac{P^2}{2I} + \cos\theta [K_1 f_1(t) + K_2 f_2(t)], \tag{8}$$

where $f_1(t)=f_1(t+T_1)$ and $f_2(t)=f_2(t+T_2)$ are smooth periodic functions of time. If $r=T_2/T_1$ is rational, the Hamiltonian (8) is periodic and DL is expected to occur. If r is an irrational number, recent experimental results [5] show that DL is destroyed or at least the localization time is increased by an order of magnitude. In view of the discussion of the preceding section, one might expect that unlimited

diffusion would result also in this case. However, as we show below, DL persists in the quasiperiodic, nonimpulsive case.

In order to fix ideas, we specify each of the driving functions as a periodic sequence of Gaussian pulses of characteristic width σ, so that for $s=1,2$

$$f_s(t)=\frac{1}{\sigma\sqrt{2\pi}}\sum_{n=-\infty}^{\infty}\exp\left[-\frac{(t-nT_s-\Phi_s)^2}{2\sigma^2}\right]. \qquad (9)$$

Without loss of generality we choose $\Phi_1=0$ and $\Phi_2=\Phi$. Thus, the driving function in Eq. (8) consists of a superposition of pulses of strength K_s that occur at times $T_1, 2T_1, \ldots$ and $\Phi+T_2, \Phi+2T_2, \ldots$. In the limit $\sigma\to 0$, the pulses reduce to δ functions and the Hamiltonian (8) reduces to Eq. (1), describing a two-frequency kicked rotor. As discussed in Sec. II, if r is irrational, this system shows diffusion for ever.

At this point, there is one important difference to bear in mind: in the classical kicked rotor, it is well known that for large K (in practice, $K\gtrsim 5$ suffices) all Kolmogorov-Arnold-Moser (KAM) surfaces are destroyed and the energy increase is unbounded [8,9]. In contrast, for finite σ, the momentum spread is limited by the existence of KAM surfaces for all values of K. However, this upper bound in momentum space increases with K in a predictable form [10]. We have checked that the classical phase space accessible in the time scales considered here is completely chaotic, so that these KAM boundaries do not affect our results.

The Schrödinger equation for the Hamiltonian (8) can be expressed in the angular momentum representation as

$$\dot{a}_n+\frac{iE_n}{\hbar}a_n+\frac{i}{2}[\kappa_1 f_1(t)+\kappa_2 f_2(t)](a_{n-1}+a_{n+1})=0. \qquad (10)$$

We have numerically integrated this equation and calculated the average energy as a function of time, for a small (but finite) pulse width σ. Our results are shown in Fig. 3, for several values of σ. As expected, they depend strongly on the rational or irrational character of the ratio $r=T_2/T_1$. In the case of two commensurable frequencies (periodic driving) the rotor localizes after a few kicks. When the two frequencies are incommensurate, the system also localizes but in a much longer time scale. The persistence of DL found here is in striking contrast with the case of impulsive driving discussed in Sec. II. The localization time for quasiperiodic driving increases as $\sigma\to 0$, approximately as σ^{-2}. We explain this dependence below, but here we note that the localization time becomes infinite in the impulsive limit.

We can understand these results by considering the Fourier transform of the driving function $f(t)=\kappa_1 f_1(t)+\kappa_2 f_2(t)$, given by

$$F(\omega)=\frac{e^{-\omega^2\sigma^2/2}}{\sigma\sqrt{2\pi}}\left[\kappa_1\sum_{m=-\infty}^{\infty}\delta(\omega-m\omega_1)+\kappa_2\sum_{n=-\infty}^{\infty}\delta(\omega-n\omega_2)\right]. \qquad (11)$$

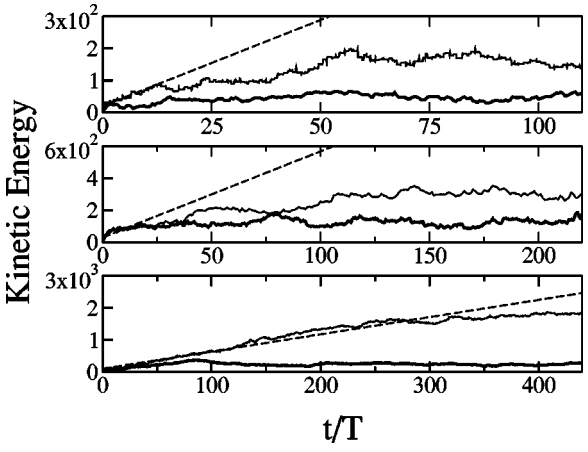

FIG. 3. Kinetic energy (units of $\hbar^2/2I$) of the quantum forced rotor described by Eq. (8) with Gaussian driving functions given by Eq. (9). Three characteristic pulse widths are shown: upper panel $\sigma/T=0.05$, medium panel $\sigma/T=0.03$, and lower panel $\sigma/T=0.01$. The other parameters are fixed at $\kappa_1=\kappa_2=3.279$ and $\xi=1.525$. The thick lines correspond to the periodic case with $r=3/2$, the thin lines to the quasiperiodic case with $r=\sqrt{2}$, and the dashed lines to the energy increase predicted by the quasilinear approximation to the classical diffusion coefficient, Eq. (5). In all cases, the initial state was a Gaussian packet in the momentum representation, centered at $\ell=0$.

The dynamical response that emerges from Eq. (10) involves the differences of the frequencies in the Fourier spectrum of the driving function $f(t)$, that is, $\omega_{nm}=|n\omega_2-m\omega_1|$. We have previously introduced these frequencies in Eq. (7). As $\sigma\to 0$ and the Gaussian modulation factor in Eq. (11) becomes unity, all harmonics of ω_1 and ω_2 are equally important in Eq. (11) and all the differences ω_{nm} appear with equal weights in the dynamical response. In this case, the frequency spectrum of the response is dense and there is no DL (see Fig. 1). For finite σ, the Gaussian modulation factor effectively suppresses all high harmonics ($\omega>1/\sigma$) from the Fourier spectrum of the driving function. Then, only a finite number of linear combinations ω_{nm} are important in the dynamical response, so the spectrum is effectively discrete and DL takes place.

The above mentioned σ^{-2} dependence of the localization time can be understood recalling that, according to the argument presented at the end of Sec. II, this time is inversely proportional to the average separation between adjacent frequencies, $\Delta\omega$. This quantity is inversely proportional to the number of significant frequencies ω_{nm} that appear in the dynamics of the system. Then, the localization time is proportional to this number of relevant frequencies. Since only $\sim 1/\sigma$ harmonics of each fundamental frequency enter in the dynamics, the number of significant frequencies ω_{nm} and the localization time, both increase as $1/\sigma^2$ as σ is reduced. We note that a similar argument has been used in the context of periodically driven systems to establish the proportionality of the localization time to the number of quasienergies that participate in the dynamics [7].

Another example of a nonimpulsive, driven quantum system is provided by a particle confined in an infinite square

well with a periodically changing width $L(t)$. This system, known as the Fermi accelerator, shows DL when its classical counterpart is chaotic [11,12]. We have considered a quasiperiodic version of this system in the context of nuclear dissipation theory and found that the localization time increases by an order of magnitude but DL still takes place [13,14]. An analysis completely analogous to the one presented above explains the persistence of DL in the quasiperiodic Fermi accelerator as a consequence of the discreteness of the effective frequency spectrum of the dynamical response.

IV. MODULATED KICKED ROTOR

In Sec. II, we have considered a kicked rotor driven by two impulsive driving functions of different frequencies and showed that DL does not take place when the frequency ratio is irrational. In contrast, in Sec. III, we presented two examples of smoothly driven quasiperiodic systems in which DL persists, although in a longer time scale than in the periodic case. We now consider an intermediate case in which the driving function has two frequencies but only one of them has an impulsive character, while the other one is associated with a smooth function of time that multiplies the impulsive term.

Two examples of such systems have been discussed in Refs. [15,16]. Here, we consider a simple periodic modulation so that the rotor is described by the Hamiltonian

$$H=\frac{P^2}{2I}+K\cos\theta\cos^2(2\pi t/T_2)\sum_{n=1}^{\infty}\delta(t-nT_1), \quad (12)$$

which corresponds to a kicked rotor with a fixed interval $T\equiv T_1$ between kicks and a kick strength modulated by a function of period T_2. We refer to the quantum version of this system as the modulated quantum kicked rotor. The map (2) is still valid in this case if the time dependent kick strength is redefined as

$$\kappa_n\equiv\kappa\cos^2(2\pi n/r). \quad (13)$$

The evolution of the energy, obtained by iterating the map (2) for the first 2000 kicks, is shown in Fig. 4. For rational r, the energy localizes as expected, since in this case the system is periodic and equivalent to a QKR. Localization is broken in the quasiperiodic case (irrational r) and, in what follows, we will focus our attention in this case. The dashed line in Fig. 4 corresponds to the quasilinear approximation to the diffusion coefficient, Eq. (5) calculated for the average value of the squared kick strength,

$$\overline{\kappa^2}\equiv\frac{1}{N}\sum_{n=1}^{N}\kappa_n^2=\frac{3}{8}\kappa^2. \quad (14)$$

The quantum diffusion, shown in Fig. 4, takes place at a slower rate than the classical one. The reason for this slower quantum diffusion rate will soon become apparent.

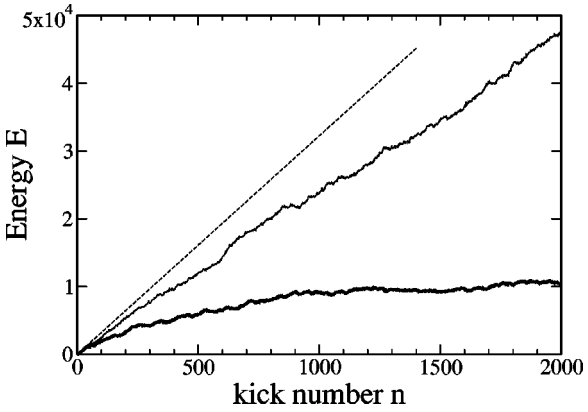

FIG. 4. Energy (in units of $\hbar^2/2I$) of the modulated quantum kicked rotor, Eq. (12), as obtained from the quantum map (2) for $\kappa-n$ given by Eq. (13). The thick line corresponds to the periodic case with $r=3/2$ and the thin line to the quasiperiodic case with $r=\sqrt{2}$. The initial state is the ground state of the unperturbed system, $|\ell=0\rangle$. The dashed line has a slope given by the quasilinear approximation to the classical diffusion coefficient, Eq. (5), with the average kicked strength from Eq. (14) . The other parameters are $\kappa=13.114$ and $\xi=1.525$.

As shown in the left panel of Fig. 5, for small values of κ the dynamics is localized. As κ is increased, the evolution of the energy shows a transition between a localized and delocalized dynamics. There is some critical value such that for $\kappa<\kappa_{crit}$, DL takes place after a characteristic time, but for $\kappa>\kappa_{crit}$ quantum diffusion persists for very long times. We have checked that the diffusion continues for at least 10^4 periods. Furthermore, as $\kappa\gg\kappa_{crit}$ the diffusion rate approximates the classical one. In fact, the same diffusion rate is obtained for a series of kicks of random strengths, obtained by replacing the ratio t/T_2 in Eq. (12) by a uniform random

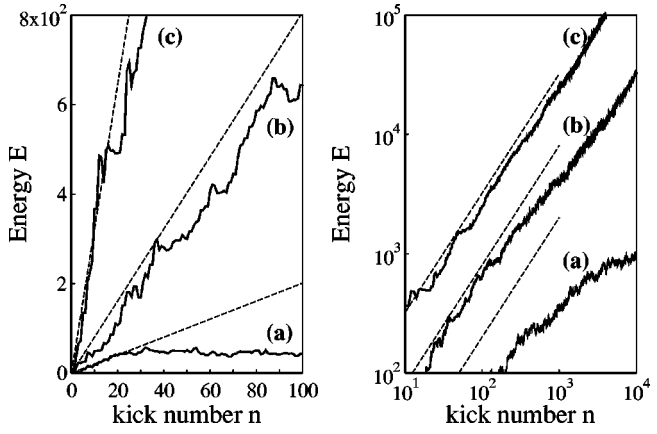

FIG. 5. Energy (units of $\hbar^2/2I$) for the modulated quantum kicked rotor as a function of kick number n for three different kick strengths: (a) $\kappa=3.28$, (b) $\kappa=6.56$, and (c) $\kappa=13.11$. The scale parameter has been fixed at $\xi=1.525$. In all cases, the dashed line corresponds to the quasilinear approximation to classical diffusion. In the right panel, the long time behavior (note the log-log scales) is given. In the left panel, the detailed short-time evolution corresponding to the boxed region in the right panel is shown in a linear scale.

variable in [0,1]. This kind of transition, between a localized and a delocalized regime, has been reported in connection with other versions of the modulated kicked rotor [15,16].

The existence of this transition, as well as the fact that the quantum diffusion rate is lower than the classical one, can both be understood from a detailed inspection of the map (2). We start by noting that since in this case $\Delta t_n = T$, the only time dependence in the coefficients in the right-hand side of (2) appears in the argument of the Bessel function. The frequencies introduced in the dynamics by this time dependence can be made explicit by recalling the definition of the Bessel function

$$J_\nu(\kappa_n) = \sum_{k=0}^{\infty} (-1)^k \frac{1}{k!(\nu+k)!} \left(\frac{\kappa_n}{2}\right)^{2k+\nu}. \qquad (15)$$

If the complex form of Eq. (13) for κ_n is substituted in Eq. (15), a series of the form $\Sigma_p c_p e^{ip\omega t}$ is obtained, in which the coefficients c_p decay at a rate that depends on κ. When this series expansion for J_ν is substituted in Eq. (6), after n kicks each frequency will introduce n harmonics in Eq. (6). More generally, if there are q relevant frequencies in Eq. (15), they introduce q^n frequencies in Eq. (6). Furthermore, when the energy is calculated from Eq. (3), these frequencies produce phases that interfere between themselves giving rise to a localized or delocalized dynamics, depending on the value of κ. An estimate of the critical value κ_{crit} can be obtained by comparing the average over several kicks, $\overline{\kappa_n/2}$, appearing in Eq. (15), with unity, so that $\kappa_{crit} \approx 4$.

This value is consistent with our numerical observations, as implied by Fig. 5. When $\kappa \gtrsim 4$, many frequencies are present with nonnegligible amplitudes in the Bessel function (15). These frequencies result in a dense response spectrum when they are ''amplified'' in Eq. (6). In this case the sums in Eq. (4) are incoherent, $\overline{\Gamma_n} \approx 0$ and quantum diffusion takes place at a rate that gradually approaches the classical one as κ is increased. On the other hand, if κ becomes smaller, the amplitudes c_p decay faster, fewer frequencies are relevant in Eq. (15) and the response spectrum has a smaller density. This produces quantum diffusion at a reduced rate as compared to the classical rate. At some value $\kappa \lesssim 4$, there is a qualitative change in the dynamics as the response spectrum undergoes a topological change from dense to discrete. Then, the sums in Eq. (3) are coherent, $\overline{\Gamma_n} = -\kappa^2/2$ and DL takes place.

V. CONCLUSIONS

All the results presented in this work can be understood in terms of the general argument presented in the last paragraph of Sec. II, based on Heisemberg's uncertainty principle. According to it, a time of the order of $1/\Delta\omega$ is required in order to resolve a separation $\Delta\omega$ in the frequency domain. In particular, when the dynamical response has a dense frequency spectrum, $\Delta\omega \to 0$, and the quantum system mimics classical diffusion for arbitrarily long times. The concrete mechanism resulting in the destruction of DL can be seen in the energy balance, Eq. (3), introduced in Sec. II. In the case of a dense frequency spectrum, the interference term of this equation is a decoherent sum of null mean value. On the other hand, when the response frequency spectrum has a discrete character, this sum is coherent and accounts for DL, as in the QKR.

We have considered three different kinds of quasiperiodically driven systems in Secs. II–IV. The differences in their dynamics can be understood in terms of the dense or discrete character of the frequency spectrum of the dynamical response.

In the two-frequency kicked rotor, considered in Sec. II, the time intervals between kicks form a dense set and this produces a dense frequency spectrum in the response. Thus, this system never localizes. In smoothly driven quasiperiodic systems, such as the rotor driven by pulses of duration σ, discussed in Sec. III, the effective frequency spectrum has a discrete character. We have shown that the average separation between frequencies, $\Delta\omega$, is in this case proportional to σ^2. Then both, the number of relevant harmonics and the localization time, increase as $1/\sigma^2$ as the impulsive limit $\sigma \to 0$ is approached. In the intermediate case of a modulated kicked rotor, presented in Sec. IV, the character of the response spectrum depends on the kick strength parameter κ. As we have discussed, this parameter determines the number of significant linear combinations of the fundamental frequencies that appear in the dynamical response. This explains the existence of a threshold ($\kappa_{crit} \sim 4$) below which DL takes place. For $\kappa \gg \kappa_{crit}$, the diffusion rate approaches the classical one.

To conclude, we have established that quasiperiodically driven systems may delocalize even in the absence of coupling with its environment. This is possible when they are driven by impulsive terms with two or more incommensurate frequencies. The additional incommensurate frequencies act as a substitute for the coupling to a noisy environment. Furthermore, we have shown that a strong causal connection exists between DL and the density of the dynamical response spectrum. This spectrum can be used to characterize the dynamics in an analogous form as the quasienergy spectrum in periodically driven systems. Finally, we have shown that the impulsive or smooth character of the driving terms of the Hamiltonian is as important for DL as the rational or irrational character of the frequency ratio.

Further work is required in order to understand how this considerations can be extended to accommodate, for example, interactions with the environment.

ACKNOWLEDGMENTS

We acknowledge the support of PEDECIBA and CONICYT-Clemente Estable (Project No. 6026). R.D. acknowledges partial financial support from MCT/FINEP/CNPq (PRONEX) under Contract No. 41.96.0886.00.

[1] G. Casati, B. V. Chirikov, F. M. Izrailev, and J. Ford, Lect. Notes Phys. **93**, 334 (1979).
[2] F. L. Moore, J. C. Robinson, C. Bharucha, P. E. Williams, and M. G. Raizen, Phys. Rev. Lett. **73**, 2974 (1994).
[3] J. C. Robinson, C. Bharucha, F. L. Moore, R. Jahnke, G. A. Georgakis, Q. Niu, M. G. Raizen, and B. Sundaram, Phys. Rev. Lett. **74**, 3963 (1995); J. C. Robinson, C. F. Bharucha, K. W. Madison, F. L. Moore, B. Sundaram, S. R. Wilkinson, and M. G. Raizen, *ibid.* **76**, 3304 (1996).
[4] H. Ammann, R. Gray, I. Shvarchuck, and N. Christensen, Phys. Rev. Lett. **80**, 4111 (1998).
[5] J. Ringot, P. Szriftgiser, J. C. Garreau, and D. Delande, Phys. Rev. Lett. **85**, 2741 (2000).
[6] F. Haake, *Quantum Signatures of Chaos*, Springer Series in Synergetics Vol. 54 (Springer-Verlag, Berlin, 1992).
[7] F. M. Izrailev, Phys. Rep. **196**, 299 (1990).
[8] E. Ott, *Chaos in Dynamical Systems* (Cambridge University Press, Cambridge, 1993).
[9] A. J. Lichtemberg and M. A. Lieberman, *Regular and Stochastic Motion* (Springer-Verlag, New York, 1983).
[10] G. Abal, R. Donangelo, A. Romanelli, A.C. Sicardi-Schifino, and R. Siri (unpublished).
[11] G. Abal, A. Romanelli, A. C. Sicardi-Schifino, R. Siri, and R. Donangelo, Physica A **257**, 289 (1998).
[12] G. Abal, A. Romanelli, A. C. Sicardi-Schifino, R. Siri, and R. Donangelo, Physica A **272**, 87 (1999).
[13] G. Abal, A. Romanelli, A. C. Sicardi Schifino, R. Siri, and R. Donangelo, Nucl. Phys. A **643**, 30 (1998).
[14] G. Abal, A. Romanelli, A. C. Sicardi Schifino, R. Siri, and R. Donangelo, Nucl. Phys. A **683**, 279 (2001).
[15] G. Casati, I. Guarneri, and D. L. Shepelyansky, Phys. Rev. Lett. **62**, 345 (1989).
[16] D. Shepelyansky, Physica D **8**, 208 (1983).